Abdominal Radiology (2019) 44:3325–3335
https://doi.org/10.1007/s00261-019-02189-8

PANCREAS

# Superparamagnetic iron-oxide-enhanced diffusion-weighted magnetic resonance imaging for the diagnosis of intrapancreatic accessory spleen

**Kousei Ishigami[1] · Akihiro Nishie[1] · Tomohiro Nakayama[1] · Yoshiki Asayama[1] · Daisuke Kakihara[1] · Nobuhiro Fujita[1] · Yasuhiro Ushijima[1] · Daisuke Okamoto[1] · Takao Ohtsuka[2] · Yasuhisa Mori[2] · Tetsuhide Ito[3] · Naoki Mochidome[4] · Hiroshi Honda[1]**

Published online: 16 August 2019
© Springer Science+Business Media, LLC, part of Springer Nature 2019

## Abstract

**Purpose** To evaluate the diagnostic performance of superparamagnetic iron-oxide (SPIO)-enhanced diffusion-weighted image (DWI) for distinguishing an intrapancreatic accessory spleen from pancreatic tumors.

**Materials and methods** Twenty-six cases of intrapancreatic accessory spleen and nine cases of pancreatic tail tumors [neuroendocrine tumor ($n=8$) and pancreatic adenocarcinoma ($n=1$)] were analyzed. Two blind reviewers retrospectively reviewed the SPIO-enhanced magnetic resonance imaging (MRI) scans. The lesion visibility grades were compared and the diagnostic performance of SPIO-enhanced DWI was compared to those of SPIO-enhanced T2WI and T2*WI with the use of a receiver operating characteristic (ROC) analysis.

**Results** The grade of lesion visibility was the highest on DWI [mean ± standard deviation (SD): $2.8 \pm 0.3$] followed by T2WI ($2.3 \pm 0.7$, $p<0.001$) and T2*WI ($2.1 \pm 0.7$, $p<0.0001$). Reviewers 1 and 2 correctly characterized the presence or absence of SPIO uptake in 34 of 35 cases (97.1%) on DWI, 24 (68.6%) and 25 (71.4%) cases on T2WI, respectively, and 16 (45.7%) and 17 (48.6%) cases on T2*WI. The area under the ROC curve (AUC) of DWI was 0.974 and 0.989 for reviewers 1 and 2, respectively. For Reviewer 1, the AUC of DWI was significantly higher than that of T2*WI (0.756, $p<0.01$), although it was not significantly different from that of T2WI (0.868, $p=0.0857$). For Reviewer 2, the AUC of DWI was significantly higher than those of T2WI (0.846, $p<0.05$) and T2*WI (0.803, $p<0.01$).

**Conclusion** The diagnostic performance of SPIO-enhanced DWI was better than those of SPIO-enhanced T2*WI and T2WI for the diagnosis of intrapancreatic accessory spleen.

**Keywords** Intrapancreatic accessory spleen · Superparamagnetic iron oxide · Diffusion-weighted image · Pancreatic tumor · Diagnostic performance

## Introduction

Accessory spleen is seen in approximately 10–30% of normal populations. Accessory spleen is most commonly seen in the splenic hilum, and the intrapancreatic location is the second most common site. According to a postmortem study [1], 61 of 364 (17%) accessory spleens were found in the pancreas. On computed tomography (CT) or magnetic resonance imaging (MRI), an intrapancreatic accessory spleen shows a round or oval mass at the edge of the pancreatic tail, with attenuation or signal intensity similar to that of the spleen [2, 3]. To avoid unnecessary surgery, an intrapancreatic accessory spleen should be distinguished from pancreatic tumors such as neuroendocrine tumors. It was also reported that intrapancreatic

✉ Kousei Ishigami
ishigami@radiol.med.kyushu-u.ac.jp

1 Department of Clinical Radiology, Graduate School of Medical Sciences, Kyushu University, 3-1-1 Maidashi, Higashi-ku, Fukuoka 812-8582, Japan

2 Surgery and Oncology, Graduate School of Medical Sciences, Kyushu University, 3-1-1 Maidashi, Higashi-ku, Fukuoka 812-8582, Japan

3 Medicine and Bioregulatory Science, Graduate School of Medical Sciences, Kyushu University, 3-1-1 Maidashi, Higashi-ku, Fukuoka 812-8582, Japan

4 Anatomic Pathology, Graduate School of Medical Sciences, Kyushu University, 3-1-1 Maidashi, Higashi-ku, Fukuoka 812-8582, Japan

accessory spleen was an important diagnostic pitfall in the diagnosis of pancreatic neuroendocrine tumors on 68 Ga-DONTAC positron emission (PET)/CT because of the high somatostatin receptor uptake in the splenic tissue [4].

The diagnosis of an intrapancreatic accessory spleen can be made noninvasively by radionuclide splenic scanning using 99mTc-labeled sulfur colloid or 99mTc-labeled heat-damaged red blood cells (RBCs) [5, 6]. Although radionuclide splenic scanning is specific, its low spatial resolution may limit the evaluation.

Superparamagnetic iron oxide (SPIO) is a reticuloendothelial system-specific contrast agent that is phagocytosed by the reticuloendothelial system in the liver, spleen, lymph nodes, and bone marrow. Intrapancreatic accessory spleen can be diagnosed using SPIO-enhanced MRI [7–9]. SPIO-enhanced MRI demonstrates negative enhancement or loss of signal intensity of an intrapancreatic accessory spleen on T2-weighted images (T2WI) or T2*-weighted images (T2*WI). However, in our clinical experience, we have noted that it not always easy to determine whether there is SPIO uptake in accessory splenic tissue.

Diffusion-weighted images (DWI) was reported to be useful for the differential diagnosis of intrapancreatic accessory spleen vs. pancreatic neuroendocrine tumor [10, 11], because the spleen has a much lower apparent diffusion coefficient (ADC) compared to the pancreas [12, 13]. Although an intrapancreatic accessory spleen is readily recognized on high *b* value DWI due to the excellent contrast to the background pancreas, high *b* value DWI does not provide direct evidence of the presence of reticuloendothelial cells.

The utility of the combination of SPIO-enhanced MRI and DWI for the detection of hepatocellular carcinoma has been reported [14], but to the best of our knowledge, the utility of SPIO-enhanced DWI for the diagnosis of an intrapancreatic accessory spleen has not been evaluated. We hypothesized that the SPIO-enhanced DWI might be a more informative diagnostic tool than SPIO-enhanced T2WI or T2*WI for the diagnosis of an intrapancreatic accessory spleen. We conducted the present study to compare the diagnostic performance of SPIO-enhanced DWI to those of SPIO-enhanced T2WI and T2*WI for the differential diagnosis of intrapancreatic accessory spleen vs. pancreatic tail tumor. If SPIO-enhanced DWI shows the best diagnostic performance as we expected, pre- and post-SPIO-enhanced DWI would be the key imaging sequences to determine the management of choice: observation (intrapancreatic accessory spleen) or surgical resection (pancreatic tumors).

## Materials and methods

### Patient population

Institutional Review Board approval was obtained, and the requirements for the patients' informed consent were waived for this retrospective study. Between May 2007 and April 2018 at our single institution, 39 patients who had had solid or mixed solid and cystic mass at the edge of the pancreatic tail underwent SPIO-enhanced MRI including DWI for the differential diagnosis of intrapancreatic accessory spleen vs. pancreatic tail tumor on a 1.5-Tesla (T) scanner. At our institution, we usually perform SPIO-enhanced MRI if contrast-enhanced dynamic CT findings are suspicious for intrapancreatic accessory spleen, because SPIO uptake represents the presence of reticuloendothelial cells in the pancreatic tail mass.

The study coordinator reviewed the diagnostic radiology report, CT and MRI images, and clinical records, and the patients were divided into intrapancreatic accessory spleen and pancreatic tumor groups. The patient population was summarized in the flow chart (Fig. 1). One post-gastrectomy patient was excluded, because the image quality was significantly degraded by metallic clips.

The histological diagnosis of intrapancreatic accessory spleen was rendered in three patients by surgical resection. In 23 patients, clinical diagnosis of intrapancreatic accessory spleen was determined by the following criteria: 1 pancreas tail mass showing similar enhancement pattern on contrast-enhanced dynamic CT; 2 morphological stability over 1 years under stable immunological environment; and 3 positive SPIO uptake on at least one of DWI, T2WI, and T2*WI (Figs. 2, 3, 4). Therefore, there were 26 patients with intrapancreatic accessory spleen.

In 12 patients, SPIO uptake was not observed in the pancreatic tail masses. Of these 12 patients, histological diagnosis was obtained in nine patients, including eight patients with pancreatic neuroendocrine tumors (Fig. 5) and one with a pancreatic ductal adenocarcinoma. The remaining three patients were lost to follow-up, and these three patients were excluded. Therefore, there were nine patients with pancreatic tail tumors.

Overall, the study group consisted of 35 patients with 35 pancreatic tail masses including 26 intrapancreatic accessory spleens and nine pancreatic tail tumors. There were 18 male and 17 female patients in the study group, ranging in age from 23 to 81 years [mean ± standard deviation (SD): 55 ± 15 years]. All 35 of the pancreatic tail masses were near the edge of the pancreatic tail. The size of the pancreatic tail masses ranged from 0.9 cm to 3.8 cm (mean ± SD: 1.9 ± 0.8 cm). Cystic change was noted in nine of the 26 intrapancreatic accessory spleens

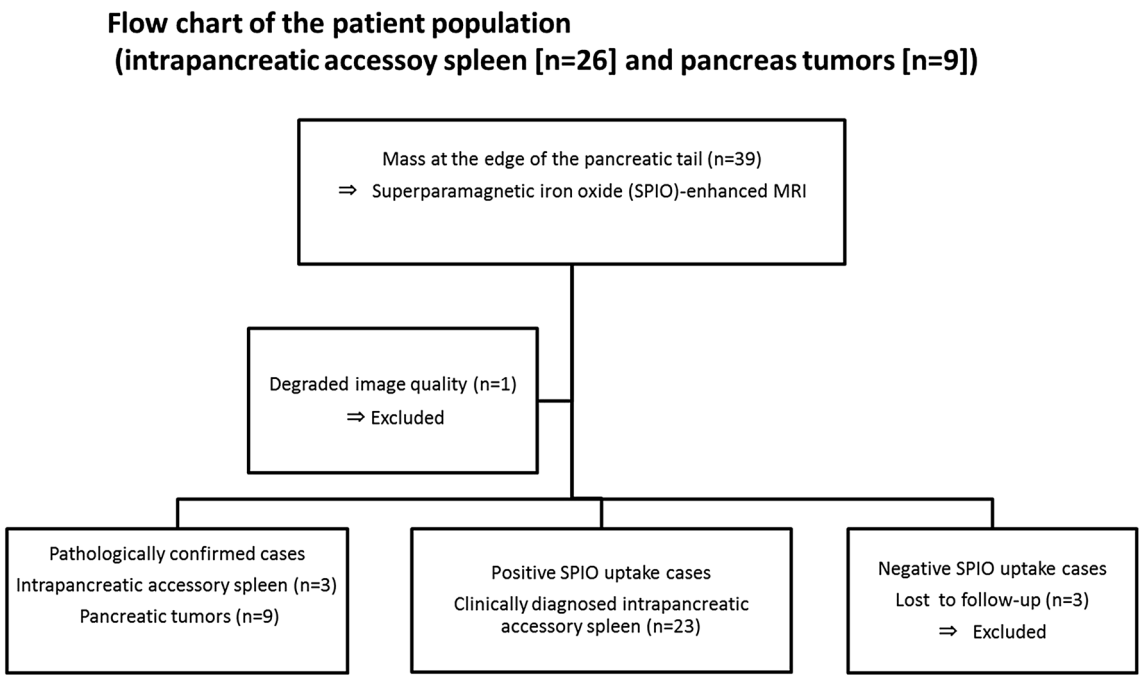


**Fig. 1** Flow chart of the patient population

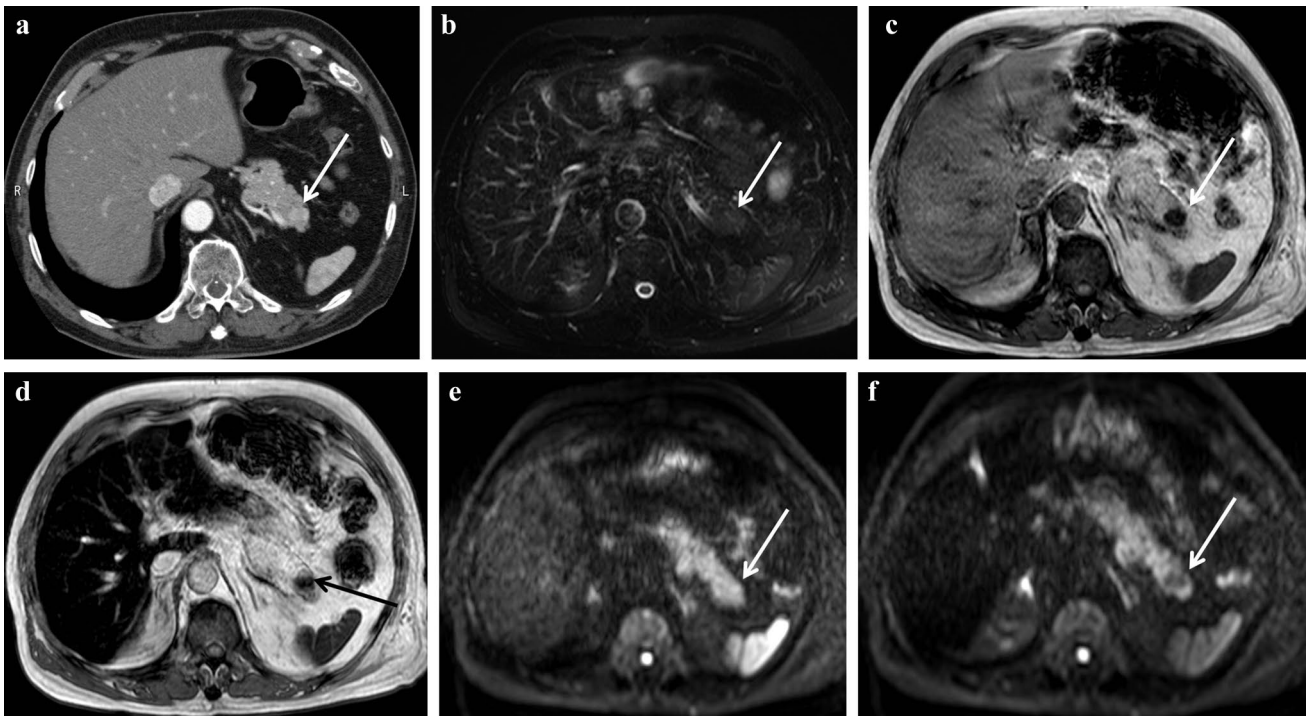


**Fig. 2** 68-year-old male with an intrapancreatic accessory spleen. **a** Pancreatic parenchymal phase of contrast-enhanced CT shows an enhancing mass in the pancreatic tail (*arrow*). **b** On this T2-weighted fast spin echo image with fat saturation (T2WI), the pancreatic tail mass is invisible (*arrow*). It was also invisible after the administration of SPIO (not shown). **c** T2*-weighted fast field echo image (T2*WI) before the SPIO administration shows a low-intensity mass in the pancreatic tail (*arrow*). **d** SPIO-enhanced T2*WI shows the low-intensity mass in the pancreatic tail (*arrow*). It is difficult to evaluate the presence or absence of SPIO uptake on T2*WI. **e** On DWI (*b* value = 1000) before the SPIO administration, the pancreatic tail mass is invisible (*arrow*). **f** On DWI (*b* value = 1000) after the SPIO administration, the pancreatic tail mass demonstrates signal loss (*arrow*), consistent with intrapancreatic accessory spleen

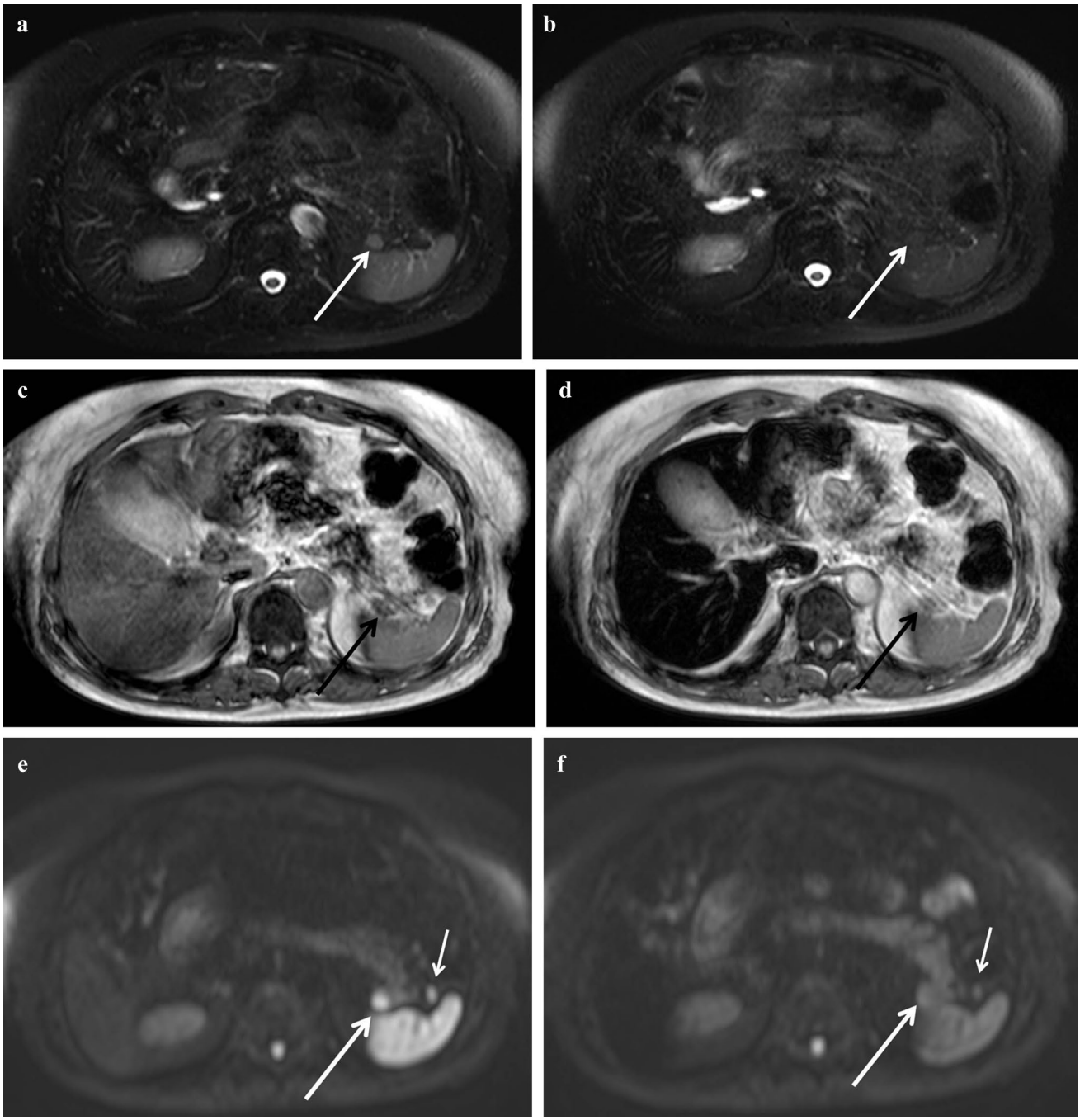


**Fig. 3** 69-year-old female with an intrapancreatic accessory spleen. **a** T2WI before the SPIO administration shows a relatively high-intensity mass in the pancreatic tail (*arrow*) with signal intensity similar to that of the spleen. **b** SPIO-enhanced T2WI shows reduction of the signal intensity in the pancreatic tail mass (*arrow*) as well as the spleen. **c** On pre-SPIO T2*WI, the pancreatic tail mass is barely visible (*arrow*). **d** On T2*WI after the SPIO administration, SPIO uptake is not clearly detected (*arrow*). The reduction of signal in the spleen is unclear compared to pre-SPIO T2*WI. **e** DWI (*b* value = 1000) before the SPIO administration clearly shows a high-intensity pancreatic tail mass (large *arrow*). *Small arrow*: Accessory spleen. **f** DWI (*b* value = 1000) after the SPIO administration clearly demonstrates the reduction of the signal in the pancreatic tail mass (*large arrow*), consistent with intrapancreatic accessory spleen. *Small arrow*: signal reduction in the accessory spleen

and five of the nine neuroendocrine tumors. The profiles of the patients with intrapancreatic accessory spleens and pancreatic tumors are summarized in Table 1.

## Imaging techniques

All MRI studies were performed with a 1.5-T MR unit (Intera Achieva Nova Dual; Philips Medical Systems,

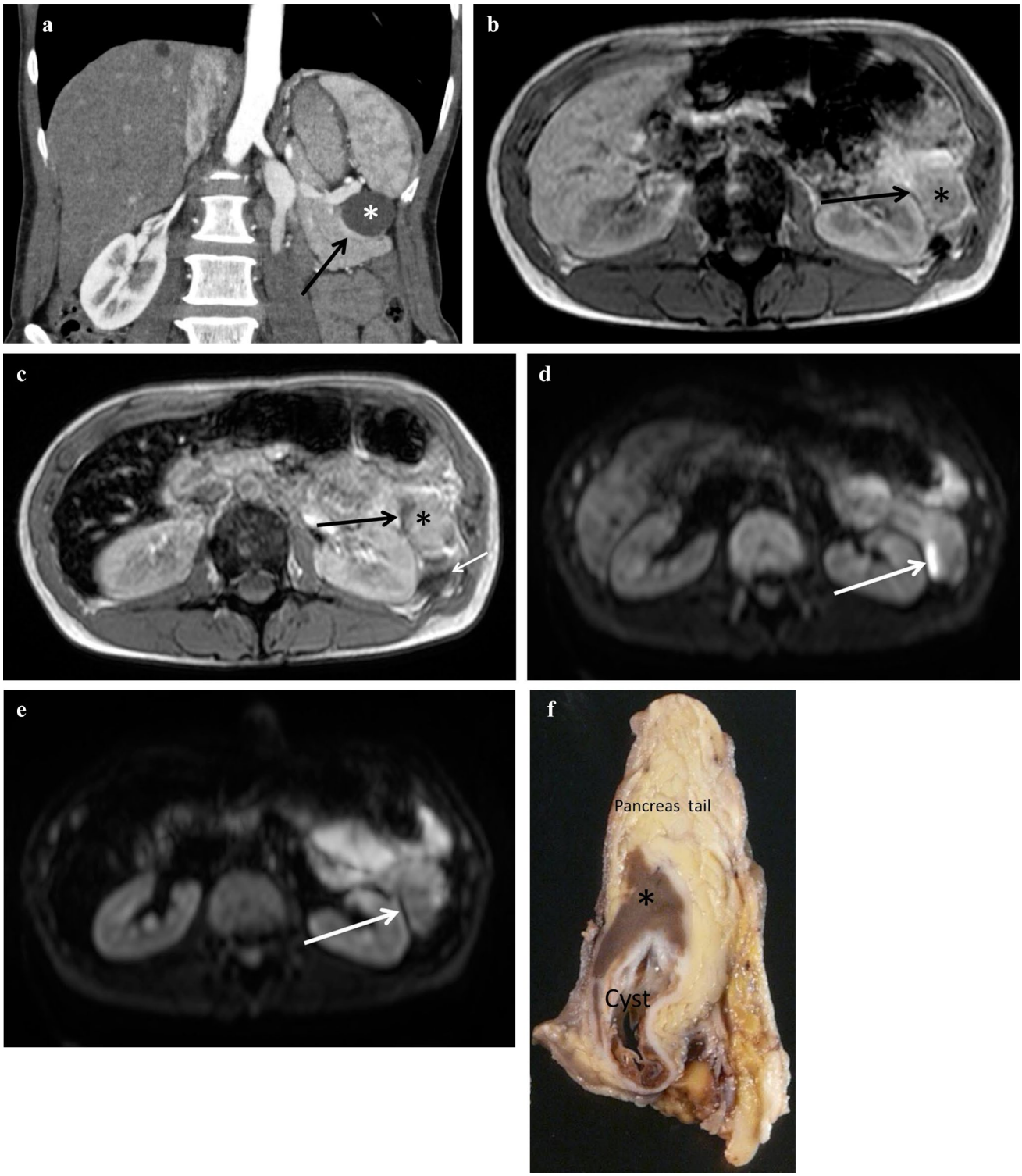


**Fig. 4** 44-year-old female with an epidermoid cyst arising from an intrapancreatic accessory spleen. **a** Coronal reformatted image of the pancreatic parenchymal phase of contrast-enhanced CT shows an exophytic cystic mass (*) arising from the edge of the pancreatic tail. Enhancing solid component (*arrow*) is noted at the inferior border of the cyst wall. **b** Pre-SPIO T2*WI shows the cystic lesion at the pancreatic tail (*asterisk*). The solid component is invisible on T2*WI (*arrow*). **c** On SPIO-enhanced T2*WI, SPIO uptake is suspected in the solid component (*large black arrow*) of the cystic lesion (*asterisk*). *Small white arrow*: the inferior edge of the spleen. On pre- and post-SPIO T2WI, the solid component was invisible (not shown). **d** DWI (*b* value = 1000) clearly shows the solid component of the pancreatic tail cyst to be high signal intensity (*arrow*). **e** Post-SPIO DWI (*b* value = 1000) shows signal loss of the solid component (*arrow*), which is more confident to assess SPIO uptake than T2*WI. **f** Resected specimen shows a brownish solid component (*asterisk*) corresponding to an accessory splenic tissue. The cystic space collapsed after formalin fixation

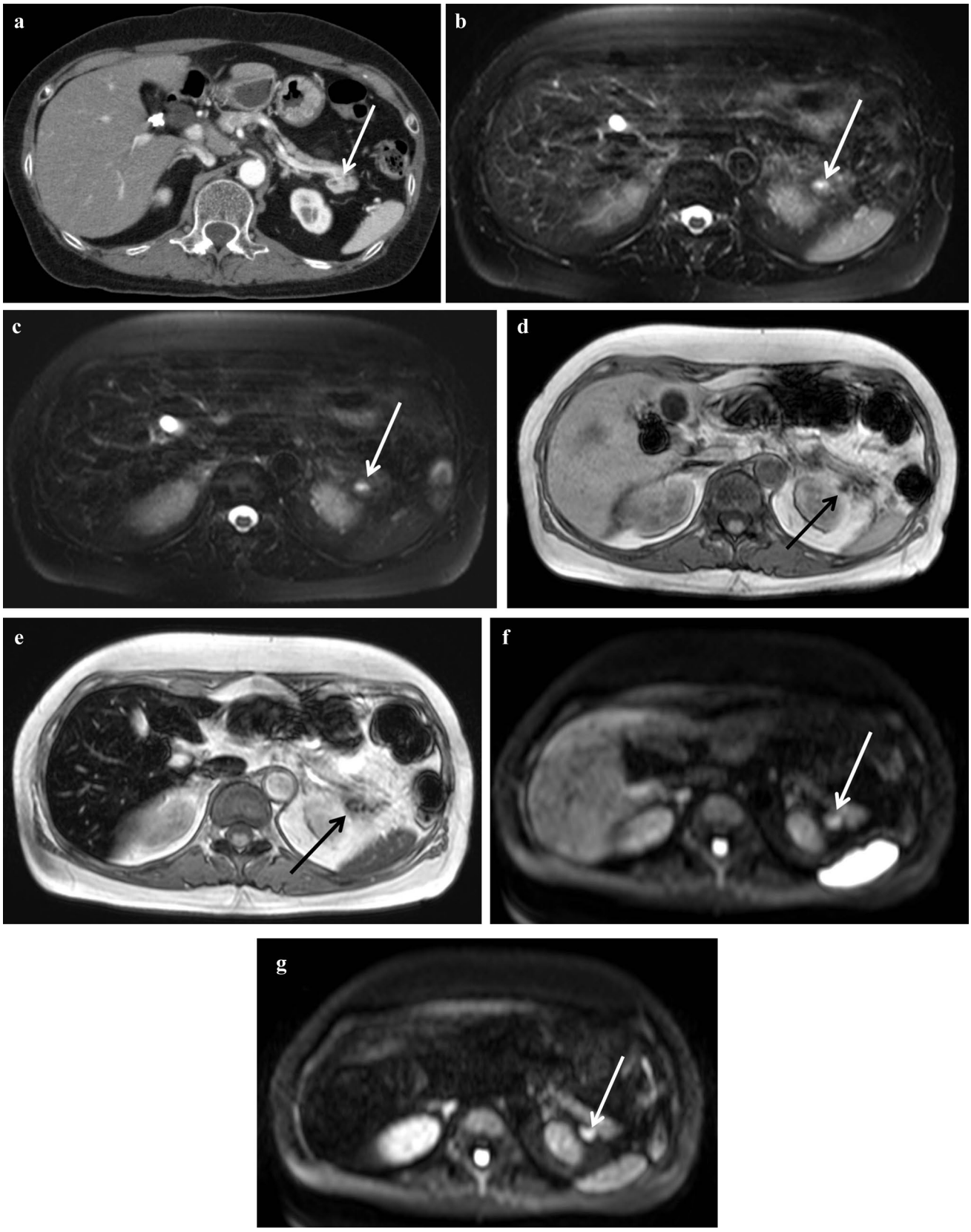
a
b
c
d
e
f
g

◂**Fig. 5** 69-year-old female with a neuroendocrine tumor of the pancreatic tail. **a** Pancreatic parenchymal phase of contrast-enhanced CT shows an enhancing mass at the edge of the pancreatic tail (*arrow*). **b** T2WI before SPIO administration shows a mixed high and intermediate signal intensity mass in the pancreatic tail (*arrow*). **c** On T2WI after SPIO administration, it is difficult to evaluate the SPIO uptake in the pancreatic tail mass (*arrow*). **d** T2*WI before SPIO administration shows the mass to be barely visible (*arrow*). **e** T2*WI after SPIO administration shows a low- intensity mass in the pancreas tail (*arrow*). It is difficult to conclude the presence or absence of SPIO uptake. **f** DWI (*b* value= 1000) before SPIO administration clearly shows a high- intensity mass (*arrow*) in the pancreatic tail. **g** DWI (*b* value= 1000) after SPIO administration shows a high-intensity pancreatic tail mass (arrow) without reduction of the signal. The lesion appears brighter than pre-SPIO image (see Fig. 4f). It is more confident to conclude the absence of SPIO uptake by DWI than T2WI and T2*WI

Best, Netherlands) equipped with a four-element sensitivity encoding (SENSE) body ($n=6$) or 32-element SENSE torso/cardiac ($n=29$) coils. Imaging included an axial dual-echo T2-weighted fast spin echo image (T2WI), axial dual-echo T1-weighted fast field echo (FFE) image (T1WI), axial dual-echo T2*-weighted FFE (T2*WI), and axial DWI. The details of the imaging parameters are summarized in Table 2.

Data acquisition was performed twice before and 10 min after an intravenous injection of 0.016 mmol Fe/kg of ferucarbotran (Resovist®; FujiFilm RI Pharma, Tokyo).

## Imaging analysis

MRI studies were retrospectively and independently reviewed by two experienced abdominal imaging radiologists who had 14 (Reviewer 1) and 19 (Reviewer 2) years of experience. The reviewers were blinded to the final diagnosis and reviewed the randomly ordered MRI studies. The reviewers assessed the lesion visibility and the presence or absence of SPIO uptake on T2WI (TR/TE= 1313/160 ms), T2*WI (TR/TE= 165/18.4 ms), and DWI (*b* value= 1000) images, separately.

The reviewers scored the lesion visibility on T2WI, T2*WI, and DWI using the following grades: 1 = invisible, 2 = visible, and 3 = clearly visible. If a pancreatic tail mass showed mixed solid and cystic components, the reviewers assessed the visibility of a solid component. Visibility score was given both to the pre- and post-SPIO images and the higher score between them was adopted to represent the patient's visibility score. For example, if a lesion was invisible on pre-SPIO images and clearly visible on post-SPIO images or vice versa, it was categorized as showing grade 3 visibility.

The reviewers assessed the presence or absence of SPIO uptake by comparing pre- and post-SPIO images on T2WI, T2*WI, and DWI. SPIO uptake was considered positive when the signal intensity of the pancreatic tail mass decreased to an intensity similar to that of the spleen. The reviewers scored their confidence level of SPIO uptake using the following grades: 1 = definitely negative; 2 = probably negative; 3 = indeterminate; 4 = probably positive; and 5 = definitely positive.

In addition, Reviewer 3 performed quantitative assessment to put the region of interest (ROI) in the solid component of the pancreatic lesions and measured the signal intensity (SI). If a solid component was invisible or too small, it was excluded from the quantitative assessment. Six, three, and one cases on T2WI, T2*WI, and DWI, respectively, were excluded, because the lesion visibility was different on each sequence. SPIO-uptake ratios on T2WI, T2*WI, and DWI were calculated by the following formula: (SI [pre-SPIO] − SI [post-SPIO])/SI (pre-SPIO).

## Data and statistical analysis

All statistical analyses were performed with EZR (Saitama Medical Center, Jichi Medical University, Saitama, Japan), which is a graphical user interface for R (The R Foundation for Statistical Computing, Vienna, Austria). More precisely, it is a modified version of R commander designed to add statistical functions frequently used in biostatistics [15].

For the lesion visibility, the average scores given by the two reviewers were recorded. The lesion visibility of the pancreatic tail lesions was compared among T2WI, T2*WI, and DWI using Wilcoxon's signed rank test.

For the diagnosis of intrapancreatic accessory spleen, if the reviewer scored the SPIO-uptake confidence level at grade 4 or 5, the diagnosis was considered correct. For the diagnosis of pancreatic tail tumors, the grades 1 and 2 were considered correct. The rates of correctly characterized cases were calculated for T2WI, T2*WI, and DWI for each of the two reviewers.

We fit the receiver operating characteristic (ROC) curves for the diagnosis of intrapancreatic accessory spleen, as the diagnostic threshold was set to grade 4 of SPIO uptake. The area under the ROC curve (AUC), sensitivity, and specificity were calculated. For each reviewer, AUCs were compared among T2WI, T2*WI, and DWI, using DeLong's test for two correlated ROC curves. The diagnostic agreement between the two reviewers was compared using kappa statistics.

For the quantitative assessment, SPIO-uptake ratios on T2WI, T2*WI, and DWI were compared between intrapancreatic accessory spleen and pancreatic tumors using Mann–Whitney *U* test. In intrapancreatic accessory spleen cases, SPIO-uptake ratios were compared among the T2WI, T2*WI, and DWI using Wilcoxon's signed rank test.

A $p$ value $< 0.05$ was considered significant.

**Table 1** Profiles of patients with intrapancreatic accessory spleen ($n=26$) and pancreatic tumors ($n=9$)

| | Intrapancreatic accessory spleen | Pancreatic tail tumors |
|---|---|---|
| Male:female | 12:14 | 6:3 |
| Age, years (mean ± SD)[a] | 23–81 (52 ± 15) | 51–78 (65 ± 10) |
| Size (mean ± SD) | 0.9–3.8 cm (1.9 ± 0.8) | 1.1–3.0 cm (1.8 ± 0.6) |
| Cystic change | 9 | 5 |

[a]The mean age of the intrapancreatic accessory spleen group is significantly younger than that of the pancreatic tail tumor group ($p=0.02$). Otherwise there were no significant differences between the two groups

## Results

### Visibility

Reviewer 1 scored grade 1 (invisible) for zero (0%) cases on DWI, six (17.1%) cases on T2WI, and 12 (34.3%) cases on T2*WI. Reviewer 2 scored grade 1 for two (5.7%) case on DWI, seven (20.0%) cases on T2WI, and seven (20.0%) cases on T2*WI. The average data of the lesion visibility of the two reviewers on DWI (mean ± SD: 2.8 ± 0.3) were significantly higher than that on T2WI (mean ± SD: 2.3 ± 0.7, $p<0.0001$) and T2*WI (mean ± SD: 2.1 ± 0.7, $p<0.0001$). In addition, the lesion visibility on T2WI was significantly higher than that on T2*WI ($p<0.05$).

### SPIO uptake

There were no indeterminate (grade 3 SPIO uptake) cases on DWI. In contrast, on T2WI, eight (22.9%) and six (17.1%) cases were considered indeterminate by Reviewers 1 and 2, respectively (Fig. 2). On T2*WI, 15 (42.9%) cases were indeterminate by both Reviewers 1 and 2 (Table 3) (Figs. 3, 5).

### Lesion characterization

The results are summarized in Table 3 (Figs. 2, 3, 4, 5). Overall, Reviewers 1 and 2 correctly characterized 34 (97.1%) of 35 cases on DWI, 24 (68.6%) and 25 (71.4%) cases on T2WI, respectively, and 16 (45.7%) and 17 (48.6%) cases on T2*WI, also respectively. The results of the ROC analysis are shown in Tables 4 and 5. For Reviewer 1, the AUC of DWI was significantly higher than that of T2*WI ($p<0.01$), although it was not significantly different from that of T2WI ($p=0.0857$). For Reviewer 2, the AUC of DWI was significantly higher than those of T2WI ($p<0.05$) and T2*WI ($p<0.01$).

The kappa values were 1, 0.689, and 0.603 on DWI, T2*WI, and T2WI, respectively. Therefore, substantial (T2WI and T2*WI) or almost perfect (DWI) agreements were achieved between Reviewers 1 and 2.

### Quantitative analysis

SPIO-uptake ratios were significantly higher in intrapancreatic accessory spleen than pancreatic tumors on DWI (mean ± SD: 0.56 ± 0.21 vs. −0.41 ± 0.44, $p<0.0001$), T2WI (0.53 ± 0.13 vs. −0.064 ± 0.12, $p<0.0001$), and T2*WI (0.32 ± 0.26 vs. 0.0072 ± 0.088, $p<0.01$). In intrapancreatic accessory spleen cases, SPIO-uptake ratios on DWI and T2WI were significantly higher than that on T2*WI ($p<0.0001$ and $p<0.01$, respectively), although there was no significant difference between DWI and T2WI ($p=0.539$). In addition, ROC analysis showed the sensitivity and specificity for the diagnosis of intrapancreatic accessory spleen to be 96% and 100%, respectively, if the threshold of the SPIO-uptake ratio on DWI was set to 0.294.

## Discussion

The diagnostic performance and the lesion visibility of T2*WI were poorer than those of T2WI and DWI. These results can be explained by the difference in the clustering of SPIO particles in the liver and spleen. The clustering of SPIO particles is more dominant in Kupffer cells in the liver than the macrophages and blood pool in the spleen [16]. The reduction of signal intensity in the spleen after SPIO administration is low on T2*WI [16, 17]. On the other hand, on T2WI, the reduction of the signal intensity of the spleen is equivalent to that of the liver [16, 17].

Our analyses demonstrated that SPIO-enhanced DWI had the best diagnostic performance for the diagnosis of intrapancreatic accessory spleen. This result was due to the excellent lesion conspicuity of intrapancreatic accessory spleens on DWI, because the spleen has the most restricted diffusion among the upper abdominal solid organs [11–13] and because the suppression of the background signals improves the conspicuity of an intrapancreatic accessory spleen.

Both pancreatic neuroendocrine tumors [18] and intrapancreatic accessory spleens can present cystic change. Epidermoid cysts may arise from an intrapancreatic accessory spleen. SPIO-enhanced MRI is useful to diagnose an epidermoid cyst arising from an intrapancreatic accessory spleen [19] if residual splenic tissue is radiologically visible as a

**Table 2** Scan parameters of MRI sequences

| | TR/TE (ms) | ETL | FA | Matrix | FOV (cm) | SENSE factor | FS | Thickness (mm) | Gap (mm) | NEX | Sections | Acquisition time |
|---|---|---|---|---|---|---|---|---|---|---|---|---|
| T2WI | 1313/80<br>1313/160 | 18 | 90° | 256 × 143 | 36 × 28.7 | 1.3 | SPIR | 6 or 8 | 1.5 or 2 | 1 | 20 | 3–5 min |
| T1WI | 165/2.3<br>165/4.6 | NA | 75° | 256 × 143 | 36 × 28.7 | 1.4 | NA | 6 or 8 | 1.5 or 2 | 2 | 20 | 18 s |
| T2*WI | 165/9.2<br>165/18.4 | NA | 75° | 256 × 143 | 36 × 28.7 | 1.4 | NA | 6 or 8 | 1.5 or 2 | 2 | 20 | 18 s |
| DWI | 2386/72 | NA | 90° | 128 × 81 | 36 × 32.6 | 2 | SPIR | 6 or 8 | 1.5 or 2 | 1 | 20 | 1–2 min |

T2WI and DWI were acquired with respiratory trigger. T1WI and T2*WI were acquired with breath hold. DWI: *b* values = 0, 500, and 1000, diffusion gradients applied in three axes, and half scan factor = 0.698

*DWI* diffusion-weighted single shot echo planar image, *ETL* echo train length, FA: flip angle, *FOV* field of view, *FS* fat saturation, *NA* not applicable, *NEX* number of excitation (signal average), *SENSE* sensitivity encoding, *SPIR* spectral pre-saturation inversion recovery, *T1WI* T1-weighted fast field echo image, *T2*WI* T2*-weighted fast field echo image, *T2WI* T2-weighted fast spin echo image, *TE* echo time, *TR* repetition time

solid component. However, SPIO-enhanced DWI may not be helpful if an epidermoid cyst appears completely cystic. Therefore, the indication of SPIO-enhanced MRI may be limited to a solid or a mixed solid and cystic lesion at the edge of the pancreatic tail.

SPIO uptake in the splenic tissue may be influenced by the phagocytic function of the reticuloendothelial cells in the splenic tissue, because there was one intrapancreatic accessory spleen case that showed false-negative SPIO uptake in our series. However, SPIO-enhanced DWI would decrease the number of such false-negative cases compared to SPIO-enhanced T2*WI and T2WI. Another expected drawback of SPIO-enhanced DWI may be the T2*-blackout of splenic tissue due to hemosiderosis.

Contrast-enhanced (CE) ultrasonography using the ultrasound contrast agent Levovist® or Sonazoid® is another tool for the diagnosis of intrapancreatic accessory spleen [20, 21], because contrast media are phagocytosed by reticuloendothelial cells. However, in some cases, the visualization of the pancreatic tail may be technically difficult by transabdominal ultrasound [22]. CE–endoscopic ultrasonography (EUS) may be a promising tool to compensate for the technical problem of transabdominal ultrasonography. However, CE–EUS may not be helpful for diagnosing a completely cystic lesion, similar to SPIO-enhanced MRI.

The diagnostic value of EUS-guided fine-needle aspiration (FNA) for an intrapancreatic accessory spleen has been equivocal. Tatas et al. [23] described that three of six (50%) intrapancreatic accessory spleens were diagnosed by EUS–FNA. Although other groups have stated that cytomorphological features and immunohistochemical staining were useful to make a diagnosis of intrapancreatic accessory spleen using EUS-guided FNA [24, 25], it is necessary to obtain sufficient biopsy samples to perform immunohistochemical staining. In addition, the role of EUS–FNA for epidermoid cysts arising from intrapancreatic accessory spleen may be limited, because the cytologic analysis of the cyst fluid is non-specific, revealing macrophages and lymphocytes, and the cyst fluid's levels of carcinoembryonic antigen (CEA) and carbohydrate antigen 19-9 (CA19-9) are usually elevated [26, 27]. SPIO-enhanced DWI is a non-invasive diagnostic tool for the diagnosis of intrapancreatic accessory spleen, and the potential risk of complications from EUS–FNA can be avoided if the SPIO uptake is positive.

A visual assessment of signal loss would be more practical in the clinical setting. However, the quantitative assessment of signal intensity supported the subjective assessment of SPIO uptake showing significant differences in SPIO-uptake ratio between intrapancreatic accessory spleen and pancreatic tumors on each MR sequence. In addition, on DWI, the mean SPIO-uptake ratio of pancreatic tumors was negative value (−0.41). According to our experience, pancreatic tumors tended to appear brighter on post-SPIO DWI,

**Table 3** Gradings of SPIO uptake and the number (percentage) of the correctly characterized cases by the two reviewers

| SPIO uptake | Grade 1 | Grade 2 | Grade 3 | Grade 4 | Grade 5 | Correctly characterized cases |
|---|---|---|---|---|---|---|
| Reviewer 1 | | | | | | |
| DWI | 7 (20.0%) | 3 (8.6%) | 0 (0%) | 4 (11.4%) | 21 (60.0%) | 34 (97.1%) |
| T2WI | 3 (8.6%) | 5 (14.3%) | 8 (22.9%) | 7 (20.0%) | 12 (34.3%) | 24 (68.6%) |
| T2*WI | 2 (5.7%) | 6 (17.1%) | 15 (42.9%) | 1 (2.9%) | 11 (31.4%) | 16 (45.7%) |
| Reviewer 2 | | | | | | |
| DWI | 4 (11.4%) | 6 (17.1%) | 0 (0%) | 9 (25.7%) | 16 (45.7%) | 34 (97.1%) |
| T2WI | 0 (0%) | 7 (20.0%) | 6 (17.1%) | 13 (37.1%) | 9 (25.7%) | 25 (71.4%) |
| T2*WI | 0 (0%) | 7 (20.0%) | 15 (42.9%) | 6 (17.1%) | 7 (20.0%) | 17 (48.6%) |

**Table 4** Sensitivity, specificity, and area under the ROC curve (AUC) for the diagnosis of intrapancreatic accessory spleen on SPIO-enhanced DWI, T2WI, and T2*WI

| | Sensitivity (%) | Specificity (%) | AUC |
|---|---|---|---|
| Reviewer 1 | | | |
| DWI | 96.2 | 100 | 0.974 |
| T2WI | 73.1 | 55.6 | 0.868 |
| T2*WI | 46.2 | 44.4 | 0.756 |
| Reviewer 2 | | | |
| DWI | 96.2 | 100 | 0.989 |
| T2WI | 76.9 | 55.6 | 0.846 |
| T2*WI | 50.0 | 44.4 | 0.803 |

For the ROC analysis, the threshold of the diagnosis of intrapancreatic accessory was set to grade 4 (probably positive SPIO uptake)

**Table 5** *p* values of the AUC among DWI, T2WI, and T2*WI by DeLong's test for two correlated ROC curves

| | Reviewer 1 | Reviewer 2 |
|---|---|---|
| DWI vs. T2WI | $p=0.0857$ | $p=0.0386$ |
| DWI vs. T2*WI | $p=0.00431$ | $p=0.00705$ |
| T2WI vs. T2*WI | $p=0.0507$ | $p=0.625$ |

For Reviewer 1, the AUC of DWI was significantly higher than that of T2*WI, although it was not significantly different from that of T2WI

For Reviewer 2, the AUC of DWI was significantly higher than those of T2WI and T2*WI

which is helpful to conclude the absence of SPIO uptake more confidently. Although the background signal loss may contribute to the signal change subjectively, it is difficult to explain why SPIO-uptake ratio of pancreatic tumors showed negative value.

SPIO has been withdrawn from the market in the United States and Europe, and it is currently available in a limited number of countries [28]. Ultra-small SPIO (USPIO) is ultimately taken up by macrophages and the reticuloendothelial system in the liver, spleen, and lymph nodes, and it has potential for imaging of the reticuloendothelial system [28, 29], including the diagnosis of intrapancreatic accessory spleen. Ferumoxytol (Feraheme®, AMAG Pharmaceuticals, United States; Rienso®, Europe) is a USPIO, which has been approved for the treatment of iron deficiency in adult chronic kidney disease patients [28]. However, it has not been utilized as an MRI contrast agent.

In our series, the mean age of the patients with intrapancreatic accessory spleen (52 years) was significantly younger than that of patients with pancreatic tumors (65 years) (Table 1). Our patient series may have included relatively younger patients incidentally found to have intrapancreatic accessory spleen, which may be a reason for the difference in the mean age of the two groups.

There are several limitations to this study. The study design was retrospective. We excluded negative SPIO-uptake cases without a pathological diagnosis ($n=3$). Although it is uncertain whether these three cases were intrapancreatic accessory spleen or pancreatic tumors, this exclusion may have caused selection bias. In addition, there was no pathological confirmation of intrapancreatic accessory spleens in 23 cases, because surgical resection is not indicated for intrapancreatic accessory spleen. The morphological stability over 1 year is not sufficient for excluding pancreatic neuroendocrine tumor. However, all clinically diagnosed intrapancreatic accessory spleen cases showed SPIO uptake. Finally, the number of pancreatic tumor cases was relatively small ($n=9$), because the indication of SPIO-enhanced MRI was based only on the clinical question for the lesions at the edge of the pancreatic tail (intrapancreatic accessory spleen vs. pancreatic tumors).

In summary, SPIO-enhanced DWI showed better diagnostic performance than SPIO-enhanced T2*WI and T2WI for the diagnosis of intrapancreatic accessory spleen due to the excellent lesion conspicuity. The addition of pre- and post-SPIO DWI is recommended to confirm the SPIO uptake for patients who are suspected to have an intrapancreatic accessory spleen.

## References


1. Halpert B, Gyorkey F. Lesions observed in accessory spleens of 311 patients. Am J Clin Pathol. 1959 Aug;32(2):165-168.
2. Harris GN, Kase DJ, Bradnock H, Mckinley MJ. Accessory spleen causing a mass in the tail of the pancreas: MR imaging findings. AJR Am J Roentgenol. 1994 Nov;163(5):1120-1.
3. Churei H, Inoue H, Nakajo M. Intrapancreatic accessory spleen: case report. Abdom Imaging. 1998 Mar-Apr;23(2):191-3.
4. Rufini V, Inzani F, Stefanelli A, et al. The Accessory Spleen Is an Important Pitfall of 68 Ga-DOTANOC PET/CT in the Workup for Pancreatic Neuroendocrine Neoplasm. Pancreas. 2017 Feb;46(2):157-163.
5. Ota T, Tei M, Yoshioka A, et al. Intrapancreatic accessory spleen diagnosed by technetium-99 m heat-damaged red blood cell SPECT. J Nucl Med. 1997 Mar;38(3):494-5.
6. Ishigami K, Hammett B, Obuchi M, et al. Imaging of an accessory spleen presenting as a slow-growing mass in the transplanted pancreas. AJR Am J Roentgenol. 2004 Aug;183(2):405-7.
7. Boraschi P1, Donati F, Volpi A, Campori G. Intrapancreatic accessory spleen: diagnosis with RES-specific contrast-enhanced MRI. AJR Am J Roentgenol. 2005 May;184(5):1712-3.
8. Herédia V, Altun E, Bilaj F, Ramalho M, Hyslop BW, Semelka RC. Gadolinium- and superparamagnetic-iron-oxide-enhanced MR findings of intrapancreatic accessory spleen in five patients. Magn Reson Imaging. 2008 Nov;26(9):1273-8.
9. Kim SH, Lee JM, Han JK, et al. MDCT and superparamagnetic iron oxide (SPIO)-enhanced MR findings of intrapancreatic accessory spleen in seven patients. Eur Radiol. 2006 Sep;16(9):1887-97.
10. Kang BK, Kim JH, Byun JH, et al. Diffusion-weighted MRI: usefulness for differentiating intrapancreatic accessory spleen and small hypervascular neuroendocrine tumor of the pancreas. Acta Radiol. 2014 Dec;55(10):1157-65.
11. Jang KM, Kim SH, Lee SJ, Park MJ, Lee MH, Choi D. Differentiation of an intrapancreatic accessory spleen from a small (<3-cm) solid pancreatic tumor: value of diffusion-weighted MR imaging. Radiology. 2013 Jan;266(1):159-67.
12. Yoshikawa T, Kawamitsu H, Mitchell DG, et al. ADC measurement of abdominal organs and lesions using parallel imaging technique. AJR Am J Roentgenol. 2006 Dec;187(6):1521-30.
13. Rosenkrantz AB, Oei M, Babb JS, Niver BE, Taouli B. Diffusion-weighted imaging of the abdomen at 3.0 Tesla: image quality and apparent diffusion coefficient reproducibility compared with 1.5 Tesla. J Magn Reson Imaging. 2011 Jan;33(1):128-35.
14. Nishie A, Tajima T, Ishigami K, et al. Detection of hepatocellular carcinoma (HCC) using superparamagnetic iron oxide (SPIO)-enhanced MRI: Added value of diffusion-weighted imaging (DWI). J Magn Reson Imaging. 2010 Feb;31(2):373-382.
15. Kanda Y. Investigation of the freely available easy-to-use software 'EZR' for medical statistics. Bone Marrow Transplant. 2013;48:452-458.
16. Tanimoto A, Oshio K, Suematsu M, Pouliquen D, Stark DD. Relaxation effects of clustered particles. J Magn Reson Imaging. 2001 Jul;14(1):72-7.
17. Gomi T, Nagamoto M, Tsunoo M, Terada S, Terada H, Kohda E. Evaluation of the changes in signals from the spleen using ferucarbotran. Radiat Med. 2007 Apr;25(3):135-8.
18. Dromain C, Déandréis D, Scoazec JY, et al. Imaging of neuroendocrine tumors of the pancreas. Diagn Interv Imaging. 2016 Dec;97(12):1241-1257.
19. Motosugi U, Yamaguchi H, Ichikawa T, et al. Epidermoid cyst in intrapancreatic accessory spleen: radiological findings including superparamagnetic iron oxide-enhanced magnetic resonance imaging. J Comput Assist Tomogr. 2010 Mar-Apr;34(2):217-22.
20. Makino Y, Imai Y, Fukuda K, et al. Sonazoid-enhanced ultrasonography for the diagnosis of an intrapancreatic accessory spleen: a case report. J Clin Ultrasound. 2011 Jul;39(6):344-7.
21. Kim SH, Lee JM, Lee JY, Han JK, Choi BI. Contrast-enhanced sonography of intrapancreatic accessory spleen in six patients. AJR Am J Roentgenol. 2007 Feb;188(2):422-8.
22. Ishigami K, Abu-Yousef DM, Kao SC, Abu-Yousef MM. Comparison of 2 oral ultrasonography contrast agents: simethicone-coated cellulose and simethicone-water rotation in improving pancreatic visualization. Ultrasound Q. 2014 Jun;30(2):135-8.
23. Tatsas AD, Owens CL, Siddiqui MT, Hruban RH, Ali SZ. Fine-needle aspiration of intrapancreatic accessory spleen: cytomorphologic features and differential diagnosis. Cancer Cytopathol. 2012 Aug 25;120(4):261-268.
24. Saunders TA, Miller TR, Khanafshar E. Intrapancreatic accessory spleen: utilization of fine needle aspiration for diagnosis of a potential mimic of a pancreatic neoplasm. J Gastrointest Oncol. 2016 Apr;7(Suppl 1):S62-5.
25. Conway AB, Cook SM, Samad A, Attam R, Pambuccian SE. Large platelet aggregates in endoscopic ultrasound-guided fine-needle aspiration of the pancreas and peripancreatic region: a clue for the diagnosis of intrapancreatic or accessory spleen. Diagn Cytopathol. 2013 Aug;41(8):661-72.
26. Kato S, Mori H, Zakimi M, et al. Epidermoid Cyst in an Intrapancreatic Accessory Spleen: Case Report and Literature Review of the Preoperative Imaging Findings. Intern Med. 2016;55(23):3445-3452.
27. Kim YS, Cho JH. Rare nonneoplastic cysts of pancreas. Clin Endosc. 2015 Jan;48(1):31-38.
28. Wang YX. Current status of superparamagnetic iron oxide contrast agents for liver magnetic resonance imaging. World J Gastroenterol. 2015 Dec 21;21(47):13400-13402.
29. Bashir MR1, Bhatti L, Marin D, Nelson RC. Emerging applications for ferumoxytol as a contrast agent in MRI. J Magn Reson Imaging. 2015 Apr;41(4):884-898.


**Publisher's Note** Springer Nature remains neutral with regard to jurisdictional claims in published maps and institutional affiliations.